Kirkuk Journal of Science Vol. 21, Iss. 2, p.64-73, 2026 doi:10.32894/kujss.2026.172294.1333

Using Heun's Method to Determine the Initial Conditions of Orbital Elements for Satellites in Low Earth Orbits

Rasha H. Ibrahim*, Zina F. Kadhim, Sura I. Gburi, H. H. AL-Dahlaki

Astronomy and Space Department, College of Science, University of Baghdad, Baghdad, Iraq.
*Corresponding author : Rasha.Ibrahim@sc.uobaghdad.edu.iq

Article Information

Article Type:
Research Article

Keywords:
Dynamic of the Orbit; eccentricity; Orbital Elements; Orbital Period of Satellite; Satellite's Perturbations.

History:
Received: 29 May 2026
Reviced: 29 June 2026
Accepted: 29 June 2026
Published Online: 30 June 2026

Citation: Rasha H. Ibrahim, Zina F. Kadhim, Sura I. Gburi and H. H. AL-Dahlaki, Using Heun's Method to Determine the Initial Conditions of Orbital Elements for Satellites in Low Earth Orbits, Kirkuk Journal of Science, 21(2), p.64-73, 2026, https://doi.org/10.32894/kujss.2026.172294.1333

Abstract

The study aims to determine the ideal starting value of eccentricity for satellites affected by atmospheric drag using Heun's method. Several altitudes from perigee were chosen for the satellites impacted by atmospheric drag. The process of transforming position and velocity components into dimensional and directional elements was described along with Heun's method. Based on the dimension and form of the orbit, the results showed that Heun's method is effective at very low values for eccentricity, less than or equal to 0.0000456. The results of the dimensional elements dropped rapidly, particularly in the next several days. The directional elements (Euler's angles) were not affected using eccentricity at any given value. Over time, the semi-major axis displays secular declining behavior, whereas the eccentricity exhibits periodic falling behavior. The results demonstrated excellent matching with previously published data using the Adams-Bashforth and Runge-Kutta methods.

1. Introduction:

In orbital mechanics, the satellite in space is identified by six orbital elements and two state vectors. During the satellite's orbital motion, it is exposed to two types of perturbations: gravitational and non-gravitational. The gravitational includes third-body attraction (this type of perturbation is due to the Sun and Moon attraction) and the non-spherical nature of the Earth (obletness, or J2).

While solar radiation pressure and atmospheric drag are examples of non-gravitational perturbations, those perturbations make the satellite drift from its real orbit; as a result, this will produce a change in the values and behavior of the state vectors and orbital elements [1, 2, 3]. Many orbit determination methods were created in the past, including a few developing techniques employing the principle of determining the state vectors, such as Gauss, Gibbs, and Lambert. These state vectors were then converted to orbital elements [4, 5].

Satellites in Low Earth Orbit (LEO) are placed between (100-1000) km with a mean Earth radius of 6378 km. Atmospheric drag causes satellites to drift away from their orbits because of the interaction between the surface of the satellite and the air molecules. The size and shape of the orbit are the most affected because they decay with time [6, 7]. Centripetal force drives the satellite inward, while centrifugal force pushes the satellite outward. Though, their influence balances out and makes the satellite maintain its orbit [8, 9]. Different numerical integration methods are suggested by researchers to find an ideal orbit.

Brito et al. studied the time necessary for the CubeSat satellite to enter the Earth under the influence of J2 and drag,

then the maximum time for staying in its orbit using numerical simulation and an analytical solution [10]. Vukovich and Kim developed models for the satellite under the influence of atmospheric drag to study the decaying prediction, allowing for the assessment of its effects. Satellites orbiting Earth follow a Keplerian orbit, but perturbations can deflect them from the classic Kepler's orbit [11]. Victor et al. simulated two small satellites in low orbit under the impact of drag to understand how solar geomagnetic activity affects satellite orbits [12].

Rasha and Abdul-Rahman used the first kind Bessel function to the value of eccentric anomaly then used Runge-Kutta's and Adams-Bashforth methods of fourth-order to investigate the deviation of orbital elements with presence of drag. A low height satellite was selected, and the results were analyzed [13]. Wu et al. investigated by the probability and behavior assessment for a space craft in a High Earth Orbit (HEO) based on Global Navigation Satellite system (GNSS) [14]. Liu et al. refined the predication of the orbit using the two-line element; also, they used a hybrid algorithm of the genetic algorithm and simplex method [15]. In this work, different altitudes in a geocentric low orbit are used under the impact of drag force only and Heun's method is used to evaluate the results.

2. Methodology:

2.1 Calculation the position and velocity components :

A position of satellite and velocity in the orbital plane can be given as [16, 17, 18]:

$$\left.\begin{aligned} x &= a(\cos\ Ec - e) \\ y &= a\sqrt{(1-e^2)}\sin\ Ec \\ z &= 0 \end{aligned}\right] \tag{1}$$

$$\left.\begin{aligned} \dot{x} &= \frac{\sqrt{(\mu_E a)}}{r} sin\ Ec \\ \dot{y} &= \frac{\sqrt{\mu_E a(1-e^2)}}{r}\cos\ Ec \\ \dot{z} &= 0 \end{aligned}\right] \tag{2}$$

Where, Ec is eccentric anomaly (this parameter is solved by the first kind of Bessel function), a is the semi-major axis (size of orbit), e is eccentricity (shape of orbit), μ_E is the gravitational constant related to Earth equal to 398600 km^3/sec^2, and r is the magnitude of the position vector. The satellite's state vectors in the equatorial plane are as follows [19, 20, 21, 22]:

$$\left.\begin{aligned} X &= G_x x + H_x y + I_x z \\ Y &= G_y x + H_y y + I_y z \\ Z &= G_z x + H_z y + I_z z \end{aligned}\right] \tag{3}$$

$$\left.\begin{aligned} X' &= G_x x' + H_x y' + I_x z' \\ Y' &= G_y x' + H_y y' + I_y z' \\ Z' &= G_z x' + H_z y' + I_z z' \end{aligned}\right] \tag{4}$$

Here,$G_X, G_Y, G_Z, H_X, H_Y, H_Z, I_X, I_Y$ andI_Z are Euler's angles.

2.2 Calculation the orbital elements:

The six orbital elements of the satellite are as follows [23, 24, 25]:

- As started, the semi-major axis is:

$$a = \left(\frac{h^2}{\mu_E} \times \frac{1}{1-e^2}\right) \tag{5}$$

Here, h is the angular momentum.

- Eccentricity (shape of orbit) is given by:

$$e = \frac{1}{\mu}\left[\left(|\mathbf{v}|^2 - \frac{\mu_E}{\mathbf{r}}\right)\mathbf{.r\text{-}(r.v).v}\right] \tag{6}$$

Where, **r** and **v** are the position and velocity vector in three dimensions.

- Inclination angle is defined as follows:

$$\cos\ i = h_Z/(h) \tag{7}$$

Where, $h_z = xy - yx$

- Right ascension of ascending node is:

$$\cos\ \Omega = N_X/N \tag{8}$$

Where, Nx is the node's line vector in (X-direction) and N: is the magnitude of this element.

- Argument of perigee formula is equally:

$$\cos\ \omega = \mathbf{N.e}/N.e \tag{9}$$

- True anomaly is determined by:

$$\cos\ \theta = \mathbf{e.r}/e.r \tag{10}$$

2.3 The perturbed acceleration:

The drag acceleration is used in this study as follows [26, 27, 28, 29]:

$$\ddot{r}_{Drag} = -\frac{1}{2} C_D \frac{A}{M} \rho \frac{\mathbf{v_r}}{\mathbf{v_r}} \tag{11}$$

Where, C_D: is parameter related to drag, A: is area, M: is mass, $\mathbf{v_r}$ is the relative velocity vector, $\mathbf{v_r}$is the magnitude in three dimensions, ρ: is the atmosphere's density, NLRMSISE-00. NRL stands for the US Naval Research Laboratory MSIS stands for mass spectrometer and incoherent scatter. E indicates that the model extends from the ground through exosphere and 00 is the year of release). An empirical atmospheric density model is used to compute this density. When there is no perturbation, the equation for the two bodies (the equation of motion) is given by [29]:

$$\ddot{r} = -\frac{\mu_E}{r^3} \mathbf{r} \tag{12}$$

2.4 Cowell's method:

As the satellite's affected by atmospheric drag, the final representation for equation of motion is obtained by adding equations (11) to (12) [30]:

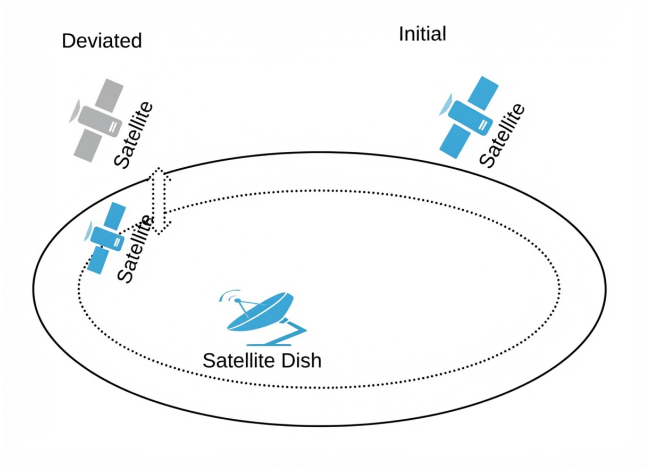

Figure 1. Illustration of the initial and deviated positions of a satellite in (LEO) [8].

$$\ddot{r}_P = -\frac{\mu_E}{r^3} r + \ddot{r}_{Drag} \tag{13}$$

Essentially, it states to add the perturbed acceleration to the unperturbed then integrated numerically gradually. This equation is a first order differential equation that results from the second order differential equation.

2.5 Numerical Integration Method (Heun's Method):

The perturbation makes the satellite deviate from its real path [28], as shown in Figure 1 [8]. It guesses the next position and velocity of the satellite depending on the initial value for position and velocity, it's advantage to integrate the acceleration and velocity to obtain a new perturbed state vectors. The equation of motion with perturbation equation (13) is integrated numerically by using the following method, which is given by [28, 29]:

$$\left.\begin{aligned} X_1 &= X_i + h(A_X) \\ Y_1 &= Y_i + h(A_Y) \\ Z_1 &= Z_i + h(A_Z) \end{aligned}\right] \tag{14}$$

$$\left.\begin{aligned} X_f &= X_1 + \frac{h}{2}(A_X) \\ Y_f &= Y_1 + \frac{h}{2}(A_Y) \\ Z_f &= Z_1 + \frac{h}{2}(A_Z) \end{aligned}\right] \tag{15}$$

Where:$A_X = \dot{X}_i, A_Y = \dot{Y}_i, A_Z = \dot{Z}_i$, h: is the time step, X_i, Y_i, Z_i and X_f, Y_f, Z_f: are the original and predicating positions in three dimensions. The equations above are to find the positions components in three dimensions. By the same method the velocities components

$$\left.\begin{aligned} X'_f &= X'_1 + \frac{h}{2}(B_X) \\ Y'_f &= Y'_1 + \frac{h}{2}(B_Y) \\ Z'_f &= Z'_1 + \frac{h}{2}(B_Z) \end{aligned}\right] \tag{16}$$

Where, X'_i, Y'_i, Z'_i and X'_f, Y'_f, Z'_f: represent the original and predicating velocities in three dimensions. Here $B_X = \ddot{r}X_o, B_Y = \ddot{r}Y_o, B_Z = \ddot{r}Z_o$.

3. Results and Discussion:

The re-evaluation of the dimensional and directional elements is used for studying the satellite's motion in its orbit. The input orbital elements are given in Table 1 [15], the MATLAB program is used to make a simulation and apply the results. It is observed that in the perturbed condition (with the presence of atmospheric drag) in Figure 2 case 1, the semi-major axis reduces as the number of orbits completes (25 days), but in the ideal condition, the semi-major axis remains constant. This element drops from 8388.69 km to 8386.75 km.

In case 2, the semi-major axis declines slowly from 7179.32 km to 7100.10 km. In case 3, it reduces by about 18 km as the number of days passes. At altitude 673 km, the behavior of

Table 1. The original orbital elements of the programs used for several satellites [28].

Orbital element	Case 1	Case 2	Case 3	Case 4	Case 5
hp (km)	576	610	571	673	507.44
a (km)	8388.0	7179.0	6959.6	7062.5	6888.6
e	0.1710234	0.0195697	0.0015196	0.0002118	0.0000456
i (deg)	88.43	35.61	82.486	98.038	31.384
Ω (deg)	219.1	273.0	260.13	166.98	191.94
ω (deg)	189.1	63.14	147.32	59.115	84.031
θ (deg)	167.3	298.9	212.48	301.02	158.65

the element that responsible for the size of the orbit is secular and reduced with time, as noticed in case 4. Finally, in case 5, it reduces gradually from 6888.68 km to 6790 km. As a result, it is noticed that the atmospheric drag pushes the satellite to be directed towards the Earth, and this leads to the shape of the orbit shrinking as compared with [8, 28, 29]. Figure 3, case 1, it is noted that eccentricity has a periodic dropping performance with different amplitudes. In case 2, it has a secularly declining behavior.

It reduces from 0.0195697 to 0.019105. In cases 3 and 4, the eccentricity continues in its periodic behavior, but with a little different amplitude. In case 5, the value of eccentricity was 0.00004, but this value dropped very slowly and periodically with a variation in amplitude as time passed. It is obviously true that the acceleration of the atmospheric drag changes the eccentricity and, likewise, the semi-major axis, which in turn leads to breaking down the line that connects the satellites with the Earth. Figure 4 depicts the resulting inclination in degrees for various initial inclination values as a function of time in days.

In case 1, the inclination has a periodic behavior that is gradually increasing with time. In case 2, the inclination reduces periodically from 35.6171° to 35.6243° with different amplitudes. The same is true in case 3, but the values of inclination angles decrease periodically and slowly as the time passes. In case 4, this orbital element is secular, dropping with time. In case 5, the inclination has a small periodic amplitude between (31.365-31.381) °, then suddenly grows 31.3847° to 31.391°.

In Figure 5 case 1, the right ascension of the ascending node starts from 219.1374°, and then increases linearly with time until it reaches the value of 285.7643°. In case 2, this element has toothed behavior. In cases 3 and 4, this element starts at 260.1351° and 166.9854°, respectively, to complete one period from (0-360) °. In case 5, this element also has toothed behavior.

In Figure 6 excluding case 4, the argument of perigee has toothed behavior, while in case 4, it has a periodic behavior between (20-120) °. Finally, through one period, the true anomaly increases from (0-360) °. In all cases and for all days, it seems toothed and starts with different values, as displayed in Figure 7 and Table 1. The results revealed a strong association when compared to previous published research [13, 27].

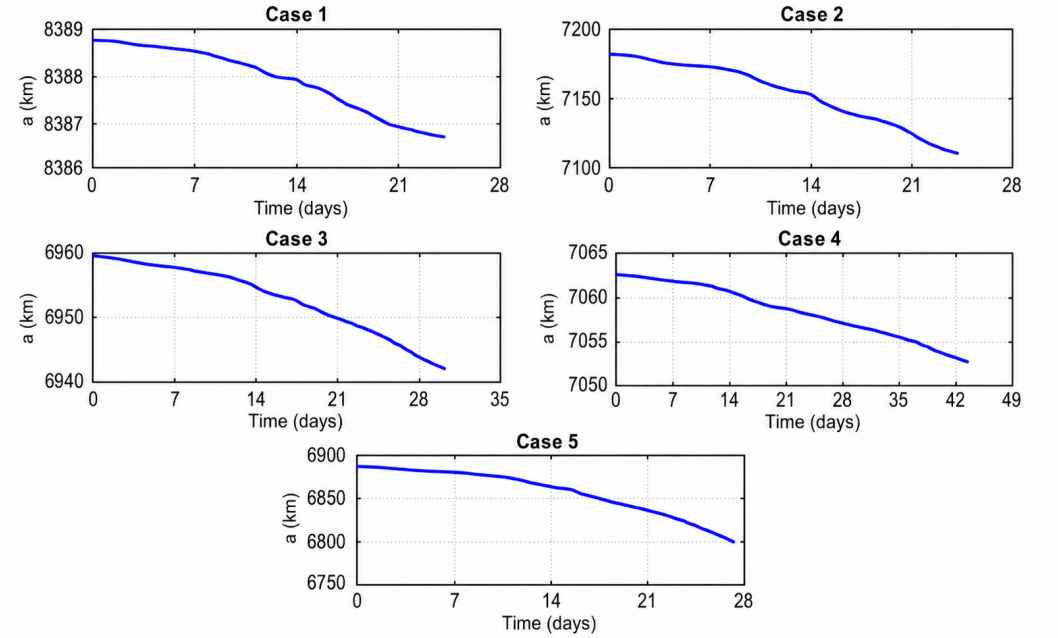

Figure 2. The resulting semi-major axis (a) in km as the time passes.

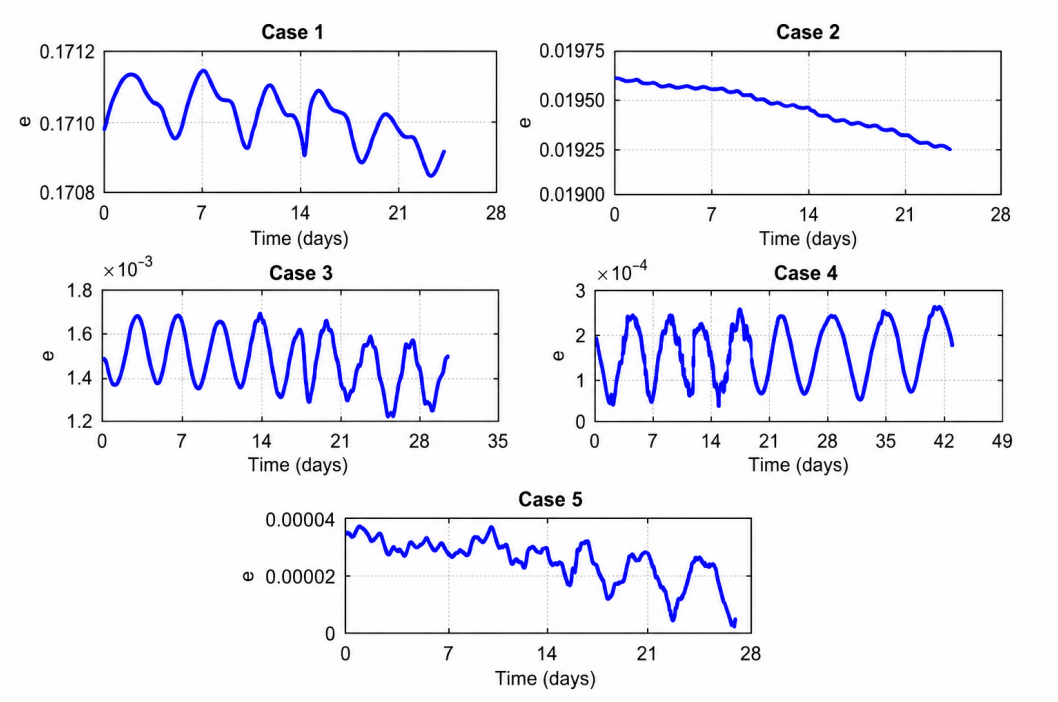

Figure 3. The resulting eccentricity (e) as the time passes.

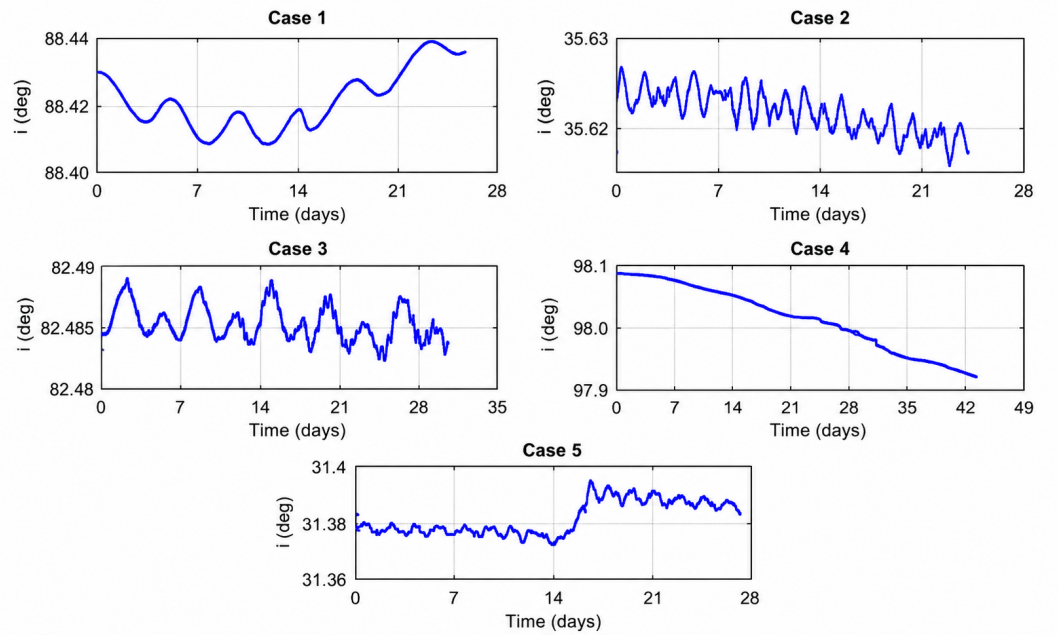

Figure 4. The resulting inclination (i) in degrees as the time passes.

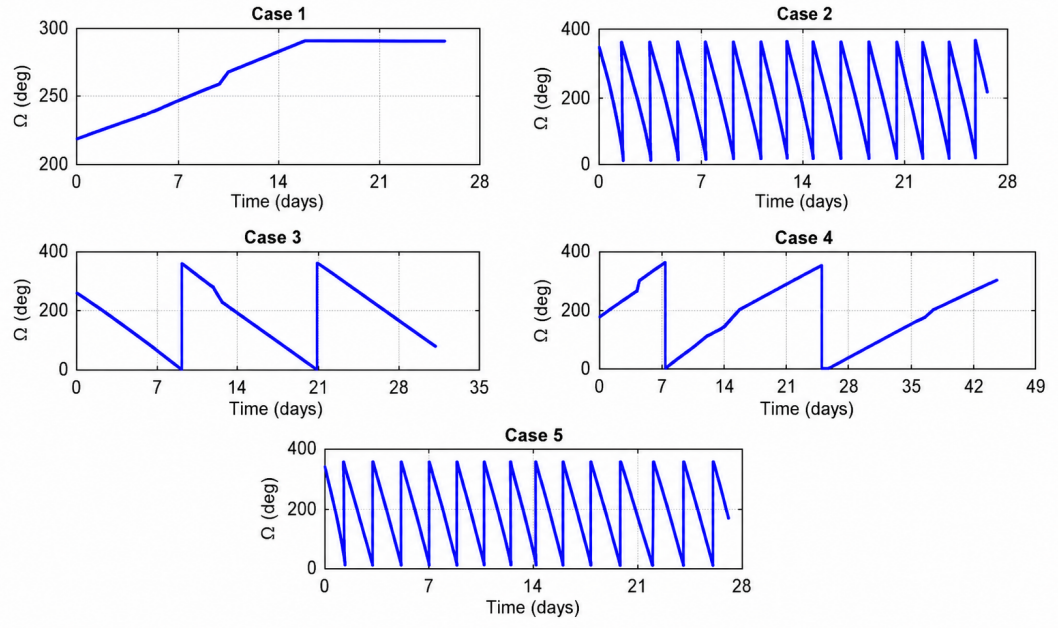

Figure 5. The resulting right ascension of the ascending node (Ω) in degrees as the time passes.

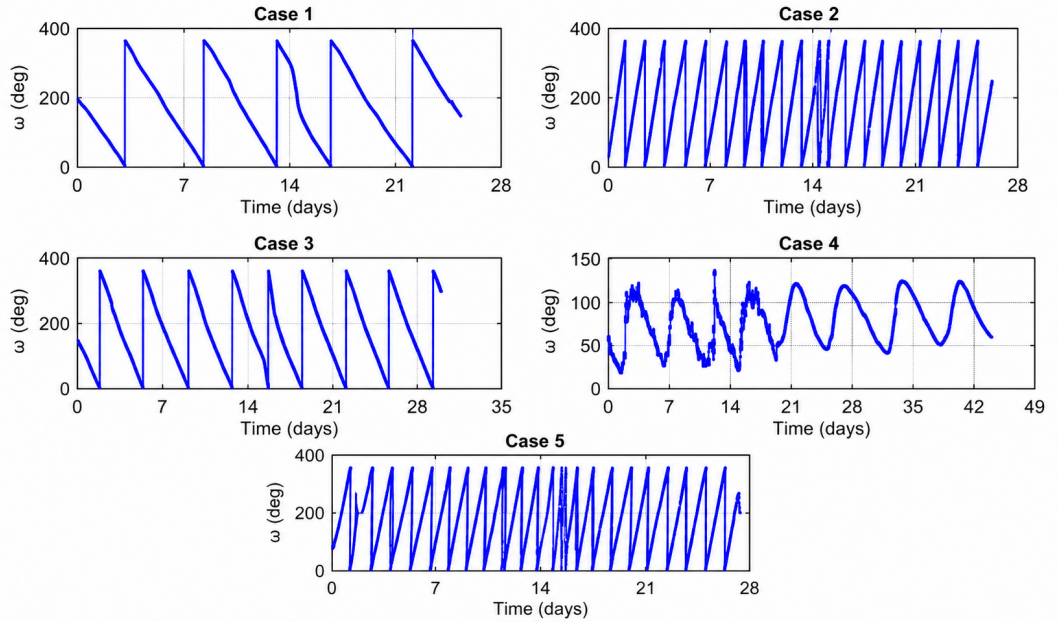

Figure 6. The resulting argument of perigee (ω) in degrees as the time passes.

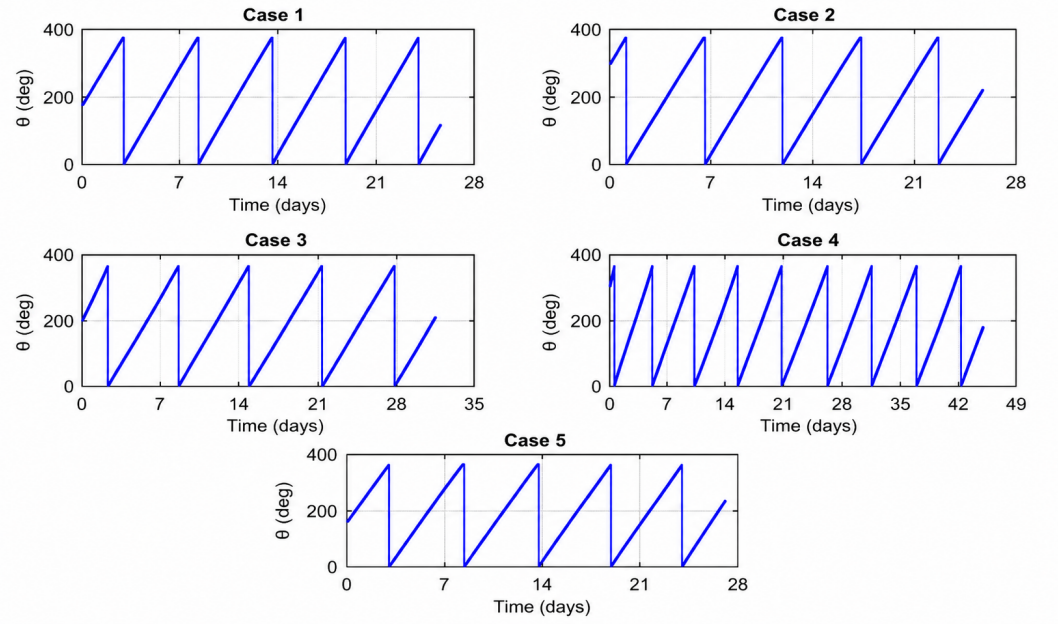

Figure 7. The resulting true anomaly (θ) in degrees as the time passes.

4. Conclusion:

Heun's method worked at very insignificant values for eccentricity, equal to or a lesser amount of than 0.0000456, based on the orbit's shape and size behavior. The two-dimensional elements (the semi-major axis and eccentricity) dropped quickly, particularly in the last several days. Eccentricity, for any given value, has no effect on the directional elements. The dimensional orbital element has a secular decreasing behavior, while the eccentricity has a periodic dropping behavior as time passes. The results showed good agreement with previously published studies that applied fourth-order Runge-Kutta and Adams-Bashforth methods.

Funding: This research received no specific grant from funding agencies in the public, commercial, or not-for-profit sector.

Data Availability Statement: All data supporting the findings of this study are available from the corresponding author upon request.

Declarations:

Conflict of interest: We hereby confirm that the document contains all of our own illustrations, tables, and diagrams.

Ethical approval: Ethical approval is not applicable for this article.

Author contributions: All authors have reviewed the final version to be published and agreed to be accountable for all aspects of the work.

References

[1] Richard H Battin. *An introduction to the mathematics and methods of astrodynamics*. Aiaa, 1999.

[2] Walter Ulrich. Astronautics the physics of space flight, 2018.

[3] Hannu Karttunen, Pekka Kröger, Heikki Oja, Markku Poutanen, and Karl Johan Donner. *Fundamental astronomy*. Springer, 6^{th} edition, 2007.

[4] Kevin Gutsche. *Precise Orbit Determination of Agile and Non-Agile Satellites*. PhD thesis, Universität Stuttgart, 12 2024, doi:10.18419/opus-15426.

[5] Lin Liu and Shengpan Zhang. *Algorithms for satellite orbital dynamics*. Springer, 2023.

[6] T. Uhlig, F. Sellmaier, and M. Schmidhuber. *Spacecraft Operations*. Springer, 01 2022, doi:10.1007/978-3-7091-1803-0.

[7] Sergey A Gutnik and Vasily A Sarychev. Symbolic-numeric simulation of satellite dynamics with aerodynamic attitude control system. In *International Workshop on Computer Algebra in Scientific Computing*, pages 214–229. Springer, 2018.

[8] S Mishra, G Singh, M Singh, and GS Gaba. Isda based precise orbit determination technique for medium earth orbit satellites. *Pertanika Journal Science and Technolgy*, 25(4):1357–1368, 2017.

[9] M Calvo, A Elipe, JI Montijano, and L Rández. Optimal starters for solving the elliptic kepler's equation. *Celestial Mechanics and Dynamical Astronomy*, 115(2):143–160, 2013, doi:10.1007/s10569-012-9456-5.

[10] TP Brito, CC Celestino, and RV Moraes. Study of the decay time of a cubesat type satellite considering perturbations due to the earth's oblateness and atmospheric drag. In *Journal of Physics: Conference Series*, volume 641, page 012026. IOP Publishing, 2015, doi:10.1088/1742-6596/641/1/012026.

[11] G Vukovich and Y Kim. Satellite orbit decay due to atmospheric drag. *International Journal of Space Science and Engineering*, 5(2):159–180, 2019, doi:10.1504/IJSPACESE.2019.10018509.

[12] Victor UJ Nwankwo, William Denig, Sandip K Chakrabarti, Muyiwa P Ajakaiye, Johnson Fatokun, Adeniyi W Akanni, Jean-Pierre Raulin, Emilia Correia, John E Enoh, and Paul I Anekwe. Atmospheric drag effects on modelled low earth orbit (leo) satellites during the july 2000 bastille day event in contrast to an interval of geomagnetically quiet conditions. In *Annales Geophysicae*, volume 39, pages 397–412. Copernicus GmbH, 2021, doi:10.5194/angeo-39-397-2021.

[13] Rasha H Ibrahim and Abdul-Rahman H Saleh. Increasing the accuracy of orbital elements for a satellite in a low earth orbit under the influence of atmospheric drag using adams-bashforth method. *Iraqi Journal of Science*, pages 81–90, 2021, doi:10.24996/ijs.2021.SI.2.9.

[14] Zhengcheng Wu, Shaojie Ni, Wei Xiao, Zongnan Li, and Huicui Liu. Study on the feasibility and performance evaluation of high-orbit spacecraft orbit determination based on gnss/slr/vlbi. *Remote Sensing*, 16(22):4214, 2024, doi:10.3390/rs16224214.

[15] Jinghong Liu, Chenyun Wu, Wanting Long, Bo Yuan, Zhengyuan Zhang, and Jizhang Sang. Improving orbit prediction of the two-line element with orbit determination using a hybrid algorithm of the simplex method and genetic algorithm. *Aerospace*, 12(6):527, 2025, doi:10.3390/aerospace12060527.

[16] Mahesh Deshmukh Kailash Malode. *Advanced Satellite Technologies*. Arcler Press, 2024.

[17] Marko Höyhtyä. *Satellite communications and networks*. Springer, 2025.

[18] Ernst Friedrich Mari Jochim. Satellite equivalence orbits. *Acta Astronautica*, 179:213–227, 2021, doi:10.1016/j.actaastro.2020.10.045.

[19] Campbell J. and Hughes S. Modern orbit determination and propagation. *NASA*, 2024.

[20] Xinyuan Mao, Wenbing Wang, and Yang Gao. Precise orbit determination for low earth orbit satellites using gnss: Observations, models, and methods. *Astrodynamics*, 8(3):349–374, 2024, doi:10.1007/s42064-023-0195-z.

[21] Mortari D. Orbit determination and estimation: Nonlinear approaches. *Springer*, 2024.

[22] Gang Zhang and Daniele Mortari. Impulsive orbit correction using second-order gauss's variational equations. *Celestial Mechanics and Dynamical Astronomy*, 132(2):13, 2020, doi:10.1007/s10569-019-9949-6.

[23] Jianjun Zhang and Jing Li. *Intelligent satellite design and implementation*. John Wiley & Sons, 2^{nd} edition, 2023.

[24] Gérard Maral, Michel Bousquet, and Zhili Sun. *Satellite communications systems: systems, techniques and technology*. John Wiley & Sons, 6^{th} edition, 2020.

[25] Oh B. Dhulipala N. Chalimadugu S. Lohmeyer W.Q., Post Ph. *Satellite Orbits Communications*. 2024.

[26] Sreekumar V.T. *Satellite Signals: Navigating the World of Satellite Communication*. 2024.

[27] Rasha H Ibrahim and Abdul-Rahman H Saleh. A comparison between runge-kutta and adems-bashforth methods for determining the stability of the satellite's orbit. In *AIP Conference Proceedings*, volume 2290, page 050002. AIP Publishing LLC, 2020, doi:10.1063/5.0027420.

[28] "Celes Trak". http://celestrak.com.

[29] Howard D.C. *Orbital Mechanics for Engineering Students*. Elsevier Aerospace Engineering Series, 3^{rd} edition, 2020.

[30] Günter Seeber. *Satellite geodesy*. Walter de gruyter, 2^{nd} edition, 2003.

استخدام طريقة هين لتحديد القيم الابتدائية للعناصر المدارية الخاصة بالاقمار الاصطناعية في الارتفاعات المنخفضة

رشا هاشم ابراهيم * ، زينة فاضل كاظم، سرى اسماعيل جبوري، حسنين حسن علي

قسم الفلك والفضاء، كلية العلوم، جامعة بغداد، بغداد، العراق.

* الباحث المسؤول: *Rasha.Ibrahim@sc.uobaghdad.edu.iq*

الخلاصة

الغرض الرئيسي من هذه الدراسة هو ايجاد أفضل قيمة ابتدائية للشذوذ المركزي باستخدام طريقة هين. استخدمت هذه الطريقة للأقمار الاصطناعية التي تتأثر باضطراب كبح الغلاف الجوي حيث تم اختيار عدة ارتفاعات من نقطة الحضيض. تم وصف عملية تحويل مركبات الموقع والسرعة الى العناصر المدارية وكذلك تم توضيح طريقة هين. أشارت النتائج بالاستناد الى حجم وشكل المدار ان طريقة هين فعالة عند قيم شذوذ مركزي قليل جدا مساوي او اقل من 0.0000456 . اشارت نتائج نصف المحور الكبير والشذوذ المركزي بأنها متناقصة وبالتحديد عند التقدم بالأيام. كانت نتائج العناصر المدارية غير متأثرة بأي قيمة للشذوذ المركزي وبمرور الوقت يكون سلوك نصف المحور الكبير متناقص بشكل خطي بينما الشذوذ المركزي يكون سلوكه متناقصا دوريا. أشارت النتائج الى تطابق جيد مع البحوث المنشورة سابقا باستخدام طريقتي آدمم باش فورث و رانج كوتا.

الكلمات الدالة: ديناميكية المدار، الشذوذ المركزي، العناصر المدارية، دورة القمر الاصطناعي، اضطرابات القمر الاصطناعي.

التمويل: لا يوجد

بيان توفر البيانات: جميع البيانات الداعمة لنتائج الدراسة المقدمة يمكن طلبها من المؤلف المسؤول.

اقرارات:

تضارب المصالح: تضارب المصالح: يقر المؤلفان بعدم وجود تضارب في المصالح

الموافقة الأخلاقية: لم تتضمن هذه الدراسة أي تجارب على البشر او الحيوانات؛ لذلك، لم تكن الموافقة الأخلاقية مطلوبة. الحصول على موافقة أخلاقية

مساهمات المؤلفين: قام جميع المؤلفين فيما بينهم بالتعاون لإكمال النسخة النهائية من جميع الجوانب.